JACS
JOURNAL OF THE AMERICAN CHEMICAL SOCIETY
pubs.acs.org/JACS
Communication

# Glutaraldehyde Cross-Linking of Oligolysines Coating DNA Origami Greatly Reduces Susceptibility to Nuclease Degradation

Frances M. Anastassacos,[‖] Zhao Zhao,[‖] Yang Zeng, and William M. Shih*

Cite This: J. Am. Chem. Soc. 2020, 142, 3311−3315
Read Online
ACCESS | Metrics & More | Article Recommendations | Supporting Information

**ABSTRACT:** DNA nanostructures (DNs) have garnered a large amount of interest as a potential therapeutic modality. However, DNs are prone to nuclease-mediated degradation and are unstable in low $Mg^{2+}$ conditions; this greatly limits their utility in physiological settings. Previously, PEGylated oligolysines were found to protect DNs against low-salt denaturation and to increase nuclease resistance by up to ∼400-fold. Here we demonstrate that glutaraldehyde cross-linking of PEGylated oligolysine-coated DNs extends survival by up to another ∼250-fold to >48 h during incubation with 2600 times the physiological concentration of DNase I. DNA origami with cross-linked oligolysine coats are non-toxic and are internalized into cells more readily than non-cross-linked origami. Our strategy provides an off-the-shelf and generalizable method for protecting DNs in vivo.



DNA nanostructures (DNs) are highly biocompatible and offer unique advantages that render them attractive candidates for therapeutics or diagnostic applications.[1−4] DNs can be programmed and folded into a great diversity of spatial conformations, and their surfaces can be functionalized by distinct guests, e.g., small molecules, proteins, nanoparticles, with nanoscale precision.[5−9] Furthermore, conformational changes triggered by environmental inputs, such as change of pH or release of specific biomolecules can be engineered into certain DNs making them responsive to different biological stimuli.[10] As such, many DNs with diagnostic and/or therapeutic potential have been reported in recent years.[11−14]

The folding of DNs requires bringing DNA helices and thus their negatively charged backbones into close proximity. This is thermodynamically unfavorable and requires high concentrations of divalent cations (most commonly, $Mg^{2+}$) to screen the electrostatic repulsion between anionic phosphate backbones. Typically, concentrations between 6 and 16 mM $MgCl_2$ are included in folding DNs, where the optimal concentration is structure dependent.[15,16] Most physiological conditions, where the total divalent cation concentration is <1 mM, represent a denaturing environment for DNs. The application of DNs in vivo is also challenged by a susceptibility to nuclease-mediated degradation.[17−19] In freshly prepared cell culture medium, RPMI with 10% FBS, the half-life of DNs is ∼12 min.[20] Furthermore, the renal clearance rate of fluorescently labeled DNs introduced by intravenous injection is similar to that of control oligonucleotides, suggesting their rapid degradation under in vivo settings. DNs must first be stabilized against low $Mg^{2+}$-based denaturation and nuclease degradation before they can be used in biomedical applications.

In recent years, these hurdles have come to the forefront of therapeutically oriented DN research with multiple approaches to improve stability (a comprehensive overview is given by Bila et al.).[21] However, most of these techniques do not offer the stability usually desired in therapeutic nanoparticles, e.g., structural integrity maintained >24 h. Furthermore, they often require specialized design considerations and cannot be applied to different structures without substantial optimization.[22,23] For example, the Dietz group has shown that cross-linking of deliberately positioned thymidines using ultraviolet irradiation can improve DN stability in low-salt conditions.[24,25] Cationic polymers and polyamines, in particular, have been shown to stabilize DNs by substituting for divalent cations.[21] Ponnuswamy et al. demonstrated that a protective coating composed of a polyamine copolymer, PEGylated oligolysine, afforded DNs a ∼400-fold increase in half-life (to ∼36 h) in media supplemented with 10% FBS.[20,21] While this technique shows a remarkable improvement in survivability, it does not yet extend the lifetime of DNs to the standards required by some biomedical applications.

PEGylated oligolysine adheres to DNs through electrostatic attraction. In low $[Mg^{2+}]$ conditions, lysines can substitute for divalent cations and neutralize the DNA-backbone electrostatic repulsions. However, since the binding between oligolysine and DNs involves a modest number of weak electrostatic interactions, it is highly dynamic and reversible. We hypothesized that covalently cross-linking amines between oligolysines would decrease mobility and/or dissociation, and thereby reduce accessibility to nucleases. Here, we show that when cross-linked with glutaraldehyde (Figure 1), PEGylated oligolysine-coated (XK10P) DNs are up to 2 orders of magnitude more resistant to nuclease degradation compared with coated DNs not treated with glutaraldehyde (K10P). This strategy has modest impact on cellular uptake of DNs and is nontoxic to mammalian cells, and therefore has potential for therapeutic purposes such as DN-based vaccines.

**Received:** November 13, 2019
**Published:** February 3, 2020





https://dx.doi.org/10.1021/jacs.9b11698
J. Am. Chem. Soc. 2020, 142, 3311−3315

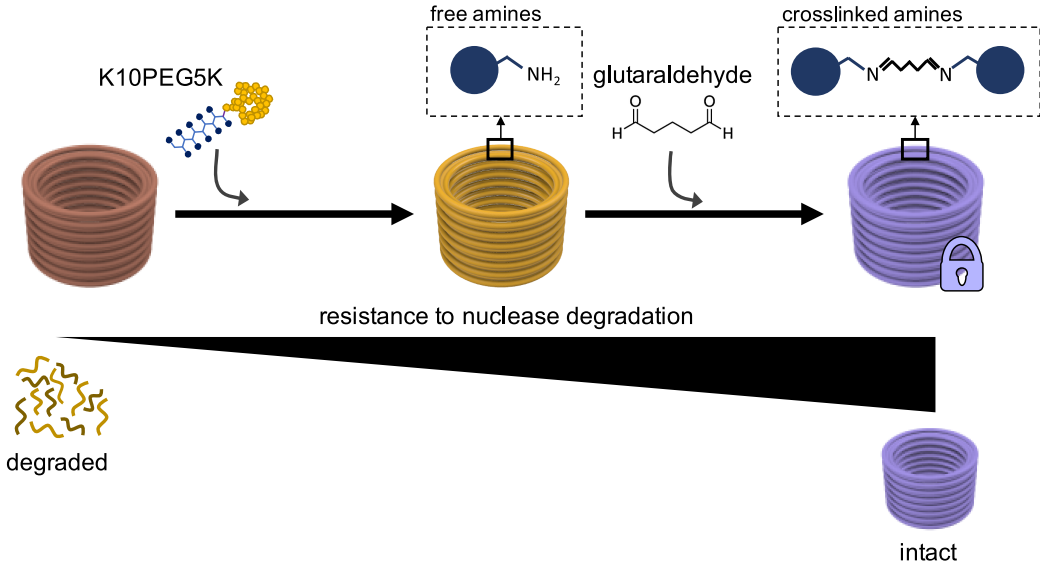


**Figure 1.** Schematic presenting the DN fabrication process and resultant increase in resistance to nuclease degradation. DNs are first coated with PEGylated oligolysine (K10P-DNs) through electrostatic adhesion. This brings primary amines in the oligolysine and DN into close proximity. This coating has been shown to increase DN resistance to nuclease degradation. Subsequent addition of glutaraldehyde covalently cross-links oligolysine amines and reduces dissociation of the lysine coating. Once cross-linked, XK10P-DNs show up to a 250-fold increase in nuclease resistance compared to un-cross-linked K10P-DNs.

We folded three structurally distinct DNs: a C-shaped DN (DN1) and two barrel-like structures with outside diameters of 90 nm (DN2) and 60 nm (DN3) (Figure 2, Figures S1–3).

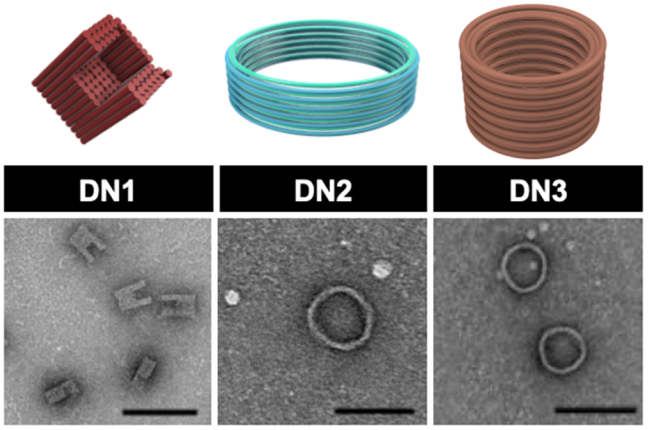


**Figure 2.** Renderings of DN1–3 and negative stain TEM images of purified structures. Scale bars, 100 nm.

DNs were designed using the software caDNAno and each folded in a one pot annealing over 18–20 h.[26] Structures were purified using glycerol gradient purification and evaluated using agarose gel electrophoresis (AGE) and negative-stain transmission electron microscopy (TEM) (Figure 2, Figure S4).

We first tested the ability of chemical cross-linkers to cross-link oligolysine and prevent release of staples from DNs. Among those investigated were known DNA cross-linkers: cisplatin and methoxypsoralen (8-MOP) as well as formaldehyde. We also tested glutaraldehyde, which has been reported not to efficiently modify DNA at moderate temperatures. As shown in Figure S5, the staples band starts to disappear on denaturing polyacrylamide gel electrophoresis (PAGE) indicating either a successful cross-linking reaction between the oligolysine and DNs staples or else cross-linking of oligolysine into networks that prevent dissociation of the staple strands. To determine whether a combination of oligolysine-PEG5K coating and cross-linking could improve the survivability of DNs when challenged with nuclease degradation, we applied the oligolysine-PEG5K coating to afford K10P-DN and then added glutaraldehyde for cross-linking (XK10P-DN) (Figure S6). Of the cross-linkers tested, glutaraldehyde showed the greatest ability to prevent DN denaturation and nuclease degradation (Figure S7).

Glutaraldehyde exists in many monomeric and polymeric forms (Figure S8). In our experiments, monomeric glutaraldehyde forms imine bonds with primary amines in the oligolysine (Figure 1), and polymeric glutaraldehyde likely forms secondary amine bonds with lysines via Michael addition to cross-link oligolysine-PEG5K molecules (Figure S7).[27] We hypothesize that this covalent conjugation decreases the mobility and dissociation of the oligolysine-PEG5K coating leading to prolonged protection of DNs. This cross-linking step appears to be generalizable to any DNA origami coated with oligolysine-PEG5K, is scalable, and can be performed without specialized equipment at room temperature. Following a short incubation at room temperature, excess cross-linker was removed using desalting columns (Zeba 7k). TEM was used to verify that no structural deformation of DNs occurs (Figure S9).

The degradation rate of DNs has been reported to be structure dependent.[15] DNase I is the prominent nuclease in blood and can be used to simulate the physiological challenge posed to DNs in an in vitro test.[15] To determine whether oligolysine-PEG5K-coated structures varied in half-life, we titrated DNase I (NEB) with various K10P-DNs and incubated reactions at 37 °C for 1.5 and 12 h. Interestingly, we found that degradation rates varied dramatically (Figure S10). To test the extent to which glutaraldehyde cross-linking of PEGylated-oligolysine coatings improves the survival of DNs, we challenged the origami with a highly strenuous nuclease


https://dx.doi.org/10.1021/jacs.9b11698
J. Am. Chem. Soc. 2020, 142, 3311–3315

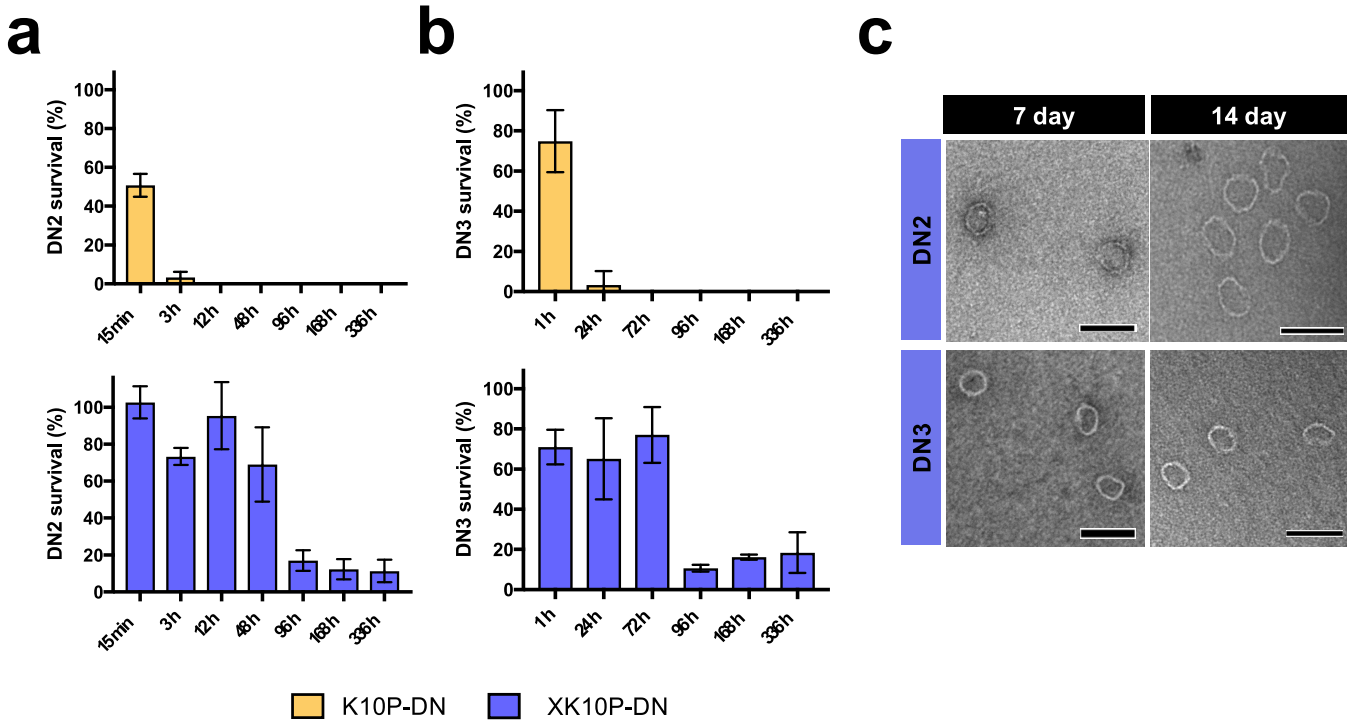


**Figure 3.** Time course of survival of DNs 2 and 3 in strenuous DNase I conditions. Normalized agarose gel intensity vs time using K10P-DN (orange) and XK10P-DN (blue) for (a) DN2 and (b) DN3. Error bars are ±SD, $n > 3$. (c) TEM images show surviving intact XK10P-DNs after incubation with 1 U/$\mu$L DNase I at 37 °C over 7 and 14 days (= 168 and 336 h, respectively). Scale bars, 100 nm.

environment of 1 U/$\mu$L DNase I. As concentrations in the blood are 340−380 U/L,[28] our conditions represent at least a 2600-fold increase in DNase I challenge. We confirmed that application of glutaraldehyde alone to DNs does not afford any protection against DNase I (Figure S11). We further confirmed that cross-linking oligolysine-coated DNs with both aged and fresh glutaraldehyde offer similar levels of protection from nuclease degradation and similar prevention of staple strand dissociation (Figure S12).

DNs were incubated with 1 U/$\mu$L DNase I at 37 °C for different time points up to 336 h (14 days). We evaluated the quantity of surviving intact structure using AGE and TEM. Under these conditions, uncoated, i.e., bare, DN survived <1 min with no intact structure observed. We observed that XK10P-DNs show a substantially increased resistance to nuclease degradation compared to K10P-DNs (Figure 3a−c). For example, K10P-DN2 showed a half-life of ∼16 min with all of the structure being completely degraded by the 3 h time-point (Figure 3a,c). However, XK10P-DN2 showed vastly extended half-lives, ∼66h, with approximately 12% of intact structure remaining even after 14 days of incubation under these conditions. This represents an ∼250-fold increase in XK10P-DN stabilization against nucleases compared to K10P-DN, based on half-life extension. We confirmed that this extended half-life could be conferred on other origami by switching to DN3 in a second set of experiments (Figure 3b−c). Additionally, we verified that prolonged incubation with XK10P-DN does not affect DNase I activity (Figure S13).

According to previously published results, under physiological conditions with 10% FBS, we expect bare DNs to have a half-life of ∼5 min, and K10P-DN3 to have a half-life of approximately 36 h.[21] We observed a 250-fold increase in stabilization compared to K10P-DN3, suggesting our strategy may enable XK10P-DNs to survive in physiological conditions with 10% FBS for over one year. However, over a long period of time, the imine bonds may hydrolyze. As a preliminary effort toward addressing this concern, we explored sodium cyanoborohydride reduction of the imine bonds formed by glutaraldehyde cross-linking of lysines. Reduction did not affect nuclease resistance in our 1 U/$\mu$L DNase I test over the course of a week (Figure S14). Future experiments can explore whether reduction impacts the long-term nuclease resistance of XK10P-DNs.

A key advantage of DNs over other nanoparticles is the ability to decorate DNs precisely with diverse cargos. This is often achieved through the Watson−Crick base-pairing of a partially embedded DNA oligonucleotide from the DN (handle) with a complementary oligonucleotide (antihandle) covalently conjugated to a cargo. To ensure that XK10P-DNs could still be loaded with cargo, we evaluated handle accessibility. We found that XK10P-DN1 is able to capture cargo after a short annealing time (Figure S15).

We next studied the interaction of our modified DNs with mammalian cells. Here, HEK293T cells diluted in standard DMEM + 10%FBS (∼0.7 mM $MgCl_2$) was used as a model system. Previous studies from our lab and others have shown the shape dependence of cellular uptake of DNs and K10P-DNs as well as the importance of scavenger-receptor-mediated and caveolin-dependent cellular uptake for DN internalization. In this study, we focus on the stability of DNs upon internalization with the goal of improving their utility as a drug delivery system or biological tool. A necessary feature that drives DNA origami toward that goal is that the system exhibits limited toxicity. We incubated a Cy5 fluorescently labeled DN3 with mammalian cells over 8 and 24 h and at different concentrations. Using flow cytometry for quantitative assessment, we monitored cell viability through membrane permeability using propidium iodide (ThermoFisher Scien-


https://dx.doi.org/10.1021/jacs.9b11698
J. Am. Chem. Soc. 2020, 142, 3311−3315

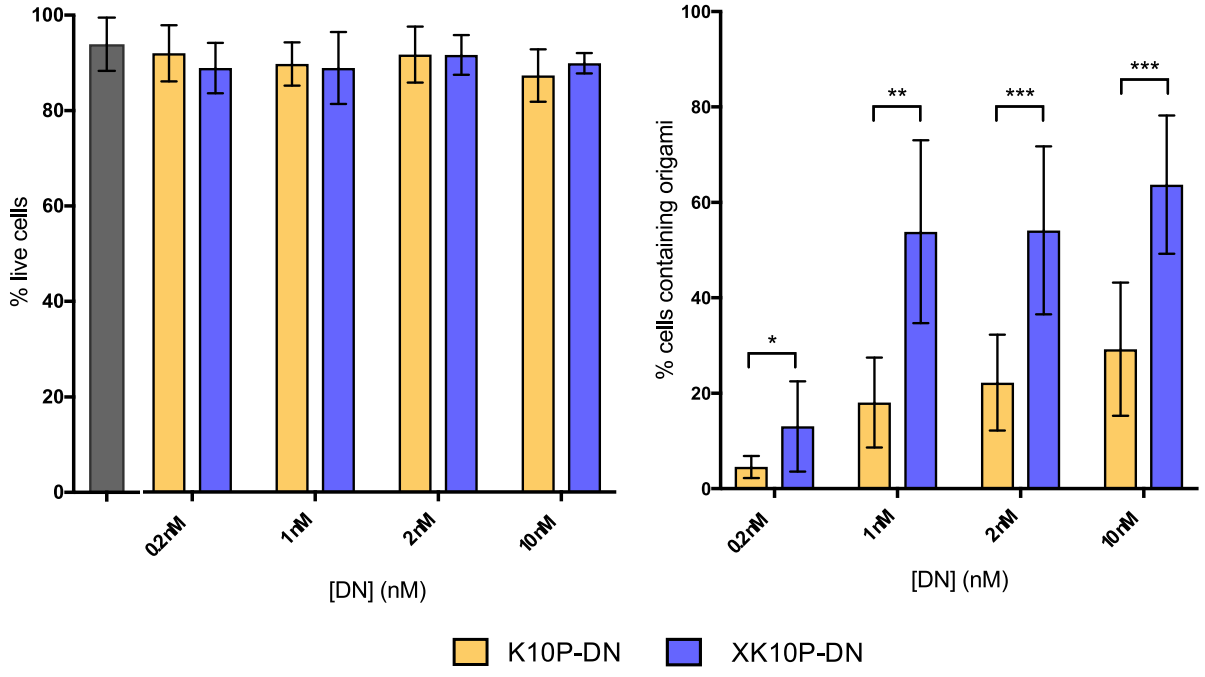


**Figure 4.** Studies of the interaction between XK10P-DNs and mammalian cells. Flow cytometry was used to study the impact of glutaraldehyde-cross-linking of DNs on (a) cell viability through labeling with membrane permeable propidium iodide and (b) cellular uptake after 24 h of HEK293T cells incubation with Cy5-fluorescent DNs. Error bars are ±SD, $n \geq 6$. * $p < 0.05$; ** $p < 0.005$; *** $p < 0.005$.

tific). No significant difference in cell viability between addition of vehicle only, K10P-DN3, and XK10P-DN3 was observed (Figure 4a, Figure S16).

Additionally, we studied the impact of the cross-linked coating on the cellular uptake of DNs, using DN3 as a model system. We observed greater cellular uptake with increasing DN concentration for both K10P-DNs and XK10P-DNs. XK10P-DN3 displayed, at each concentration, statistically significantly superior uptake compared to K10P-DN3 after 24 h of incubation (Figure 4b, Figure S17). For example, for 10 nM DN incubation with HEK293T cells, we observed over twice the uptake for XK10P-DN3 compared to K10P-DN3($p < 0.0005$). However, cellular uptake for K10P-DN3 and XK10P-DN3 after 8 h was similar (Figure S18).

A possible explanation for this discrepancy between 8 and 24 h results may be the progressive degradation of K10P-DN3 to form more amorphous structures compared to stable XK10P-DN3. We observed in previous studies that compact DNs are more efficiently uptaken by HEK293 cells.[29] Over prolonged incubations, such as 24 h incubations, this degradation could be responsible for the decreased uptake observed for K10P-DNs compared to XK10P-DNs. Since higher uptake rates are typically linked to greater biological effects, cross-linking of oligolysine coatings may assist in increasing efficacy of DN-mediated drug delivery to cells.

In conclusion, we have developed an inexpensive, scalable, and generalizable method for protecting DNs in vivo that drastically increases the nuclease resistance of DNs: Once coated with an oligolysine-PEG copolymer, amines in the oligolysines can be covalently cross-linked to increase the half-life of the underlying DN under attack by nucleases. In particular, we showed that glutaraldehyde-mediated chemical cross-linking of oligolysine-PEG5K-coated DNs increases DNs resistance to DNase I degradation under strenuous conditions up to 100,000-fold compared to bare DNs and over 250-fold compared to DNs coated with oligolysine-PEG5K but not subjected to cross-linking. We also observed a statistically significant increase in cellular uptake for XK10P-DNs compared with K10P-DNs. We believe this method is compatible with therapeutic applications since it is non-toxic and allows for the continued decoration of DNs with various surface ligands.

## ■ ASSOCIATED CONTENT

### Supporting Information

The Supporting Information is available free of charge at https://pubs.acs.org/doi/10.1021/jacs.9b11698.

Supporting experimental procedures, caDNAno illustrations of DN designs, and supporting experimental data (PDF)

## ■ AUTHOR INFORMATION


### Corresponding Author

**William M. Shih** − *Department of Biological Chemistry and Molecular Pharmacology, Harvard Medical School, Boston, Massachusetts 02115, United States;* orcid.org/0000-0002-1395-9267; Email: William_Shih@dfci.harvard.edu

### Authors

**Frances M. Anastassacos** − *Department of Cancer Biology, Dana-Farber Cancer Institute, Boston, Massachusetts 02215, United States*

**Zhao Zhao** − *Wyss Institute for Biologically Inspired Engineering at Harvard, Boston, Massachusetts 02115, United States*

**Yang Zeng** − *Department of Cancer Biology, Dana-Farber Cancer Institute, Boston, Massachusetts 02215, United States*

Complete contact information is available at: https://pubs.acs.org/10.1021/jacs.9b11698




https://dx.doi.org/10.1021/jacs.9b11698
J. Am. Chem. Soc. 2020, 142, 3311−3315

### Author Contributions

[‖]F.M.A. and Z.Z. contributed equally to this study. F.M.A., Z.Z., and W.M.S. designed the study. F.M.A. and Z.Z. produced the DNA nanostructures. Z.Z. performed initial screening of chemical cross-linkers. F.M.A. performed nuclease degradation and cell studies. Y.Z. assisted in flow cytometry and cell studies. F.M.A, Z.Z., and W.M.S. wrote the manuscript.

### Notes

The authors declare the following competing financial interest(s): The Harvard University Office of Technology Development has filed a patent application on technologies described herein.

## ■ ACKNOWLEDGMENTS

The authors thank Erika Siren and Isaac Han for contributing cell lines and expertise in mammalian cell culture and Jaeseung Hahn and Leo Chou for their helpful discussions. This work was supported by Wyss Institute for Biologically Inspired Engineering at Harvard and an NSF Expeditions award (CCF-1317291) to W.M.S. The work was further supported by the Intramural Research Program of KIST to W.M.S. and Y.Z. F.M.A. was supported by an Alexander S. Onassis Scholarship for Hellenes.

## ■ REFERENCES

(1) Li, S.; Jiang, Q.; Liu, S.; Zhang, Y.; Tian, Y.; Song, C.; Wang, J.; Zou, Y.; Anderson, G. J.; Han, J. Y.; Chang, Y.; Liu, Y.; Zhang, C.; Chen, L.; Zhou, G.; Nie, G.; Yan, H.; Ding, B.; Zhao, Y. A DNA nanorobot functions as a cancer therapeutic in response to a molecular trigger in vivo. *Nat. Biotechnol.* **2018**, *36*, 258−264.

(2) Jiang, D.; Ge, Z.; Im, H. J.; England, C. G.; Ni, D.; Hou, J.; Zhang, L.; Kutyreff, C. J.; Yan, Y.; Liu, Y.; Cho, S. Y.; Engle, J. W.; Shi, J.; Huang, P.; Fan, C.; Yan, H.; Cai, W. DNA origami nanostructures can exhibit preferential renal uptake and alleviate acute kidney injury. *Nat. Biomed Eng.* **2018**, *2*, 865−877.

(3) Tasciotti, E. Smart cancer therapy with DNA origami. *Nat. Biotechnol.* **2018**, *36*, 234−235.

(4) Hu, Q.; Li, H.; Wang, L.; Gu, H.; Fan, C. DNA Nanotechnology-Enabled Drug Delivery Systems. *Chem. Rev.* **2018**, *119*, 6459−6506.

(5) Andersen, E. S.; Dong, M.; Nielsen, M. M.; Jahn, K.; Subramani, R.; Mamdouh, W.; Golas, M. M.; Sander, B.; Stark, H.; Oliveira, C. L.; Pedersen, J. S.; Birkedal, V.; Besenbacher, F.; Gothelf, K. V.; Kjems, J. Self-assembly of a nanoscale DNA box with a controllable lid. *Nature* **2009**, *459*, 73−76.

(6) Saccà, B.; Meyer, R.; Erkelenz, M.; Kiko, K.; Arndt, A.; Schroeder, H.; Rabe, K. S.; Niemeyer, C. M. Orthogonal Protein Decoration of DNA Origami. *Angew. Chem.* **2010**, *122*, 9568−9573.

(7) Rothemund, P. W. K. Folding DNA to create nanoscale shapes and patterns. *Nature* **2006**, *440*, 297−302.

(8) Douglas, S. M.; Dietz, H.; Liedl, T.; Högberg, B.; Graf, F.; Shih, W. M. Self-assembly of DNA into nanoscale three-dimensional shapes. *Nature* **2009**, *459*, 414−418.

(9) Li, J.; Pei, H.; Zhu, B.; Liang, L.; Wei, M.; He, Y.; Chen, N.; Li, D.; Huang, Q.; Fan, C. Self-assembled multivalent DNA nanostructures for noninvasive intracellular delivery of immunostimulatory CpG oligonucleotides. *ACS Nano* **2011**, *5*, 8783−8789.

(10) Liu, M.; Fu, J.; Hejesen, C.; Yang, Y.; Woodbury, N. W.; Gothelf, K.; Liu, Y.; Yan, H. A DNA tweezer-actuated enzyme nanoreactor. *Nat. Commun.* **2013**, *4*, 2127.

(11) Douglas, S. M.; Bachelet, I.; Church, G. M. A logic-gated nanorobot for targeted transport of molecular payloads. *Science* **2012**, *335*, 831−834.

(12) Banerjee, A.; Bhatia, D.; Saminathan, A.; Chakraborty, S.; Kar, S.; Krishnan, Y. Controlled release of encapsulated cargo from a DNA icosahedron using a chemical trigger. *Angew. Chem., Int. Ed.* **2013**, *52*, 6854−6857.

(13) Linko, V.; Ora, A.; Kostiainen, M. A. DNA Nanostructures as Smart Drug-Delivery Vehicles and Molecular Devices. *Trends Biotechnol.* **2015**, *33*, 586−594.

(14) Hu, Y.; Chen, Z.; Zhang, H.; Li, M.; Hou, Z.; Luo, X.; Xue, X. Development of DNA tetrahedron-based drug delivery system. *Drug Delivery* **2017**, *24*, 1295−1301.

(15) Hahn, J.; Wickham, S. F. J.; Shih, W. M.; Perrault, S. D. Addressing the instability of DNA nanostructures in tissue culture. *ACS Nano* **2014**, *8*, 8765−8775.

(16) Kielar, C.; Xin, Y.; Shen, B.; Kostiainen, M. A.; Grundmeier, G.; Linko, V.; Keller, A. On the Stability of DNA Origami Nanostructures in Low-Magnesium Buffers. *Angew. Chem., Int. Ed.* **2018**, *57*, 9470−9474.

(17) Conway, J. W.; McLaughlin, C. K.; Castor, K. J.; Sleiman, H. DNA nanostructure serum stability: greater than the sum of its parts. *Chem. Commun.* **2013**, *49*, 1172.

(18) Mei, Q.; Wei, X.; Su, F.; Liu, Y.; Youngbull, C.; Johnson, R.; Lindsay, S.; Yan, H.; Meldrum, D. Stability of DNA origami nanoarrays in cell lysate. *Nano Lett.* **2011**, *11*, 1477−1482.

(19) Surana, S.; Bhatia, D.; Krishnan, Y. A method to study in vivo stability of DNA nanostructures. *Methods* **2013**, *64*, 94−100.

(20) Ponnuswamy, N.; Bastings, M. M. C.; Nathwani, B.; Ryu, J. H.; Chou, L. Y. T.; Vinther, M.; Li, W. A.; Anastassacos, F. M.; Mooney, D. J.; Shih, W. M. Oligolysine-based coating protects DNA nanostructures from low-salt denaturation and nuclease degradation. *Nat. Commun.* **2017**, *8*, 15654.

(21) Bila, H.; Kurisinkal, E. E.; Bastings, M. M. C. Engineering a stable future for DNA-origami as a biomaterial. *Biomater. Sci.* **2019**, *7*, 532−541.

(22) Mikkilä, J.; Eskelinen, A. P.; Niemelä, E. H.; Linko, V.; Frilander, M. J.; Törmä, P.; Kostiainen, M. A. Virus-Encapsulated DNA Origami Nanostructures for Cellular Delivery. *Nano Lett.* **2014**, *14*, 2196−2200.

(23) Perrault, S. D.; Shih, W. M. Virus-Inspired Membrane Encapsulation of DNA Nanostructures To Achieve In Vivo Stability. *ACS Nano* **2014**, *8*, 5132−5140.

(24) Gerling, T.; Kube, M.; Kick, B.; Dietz, H. Sequence-programmable covalent bonding of designed DNA assemblies. *Sci. Adv.* **2018**, *4*, No. eaau1157.

(25) Gerling, T.; Dietz, H. Reversible Covalent Stabilization of Stacking Contacts in DNA Assemblies. *Angew. Chem., Int. Ed.* **2019**, *58*, 2680−2684.

(26) Douglas, S. M.; Marblestone, A. H.; Teerapittayanon, S.; Vazquez, A.; Church, G. M.; Shih, W. M. Rapid prototyping of 3D DNA-origami shapes with caDNAno. *Nucleic Acids Res.* **2009**, *37*, 5001−5006.

(27) Migneault, I.; Dartiguenave, C.; Bertrand, M. J.; Waldron, K. C. Glutaraldehyde: behavior in aqueous solution, reaction with proteins, and application to enzyme crosslinking. *BioTechniques* **2004**, *37* (5), 790−796.

(28) Cherepanova, A.; Tamkovich, S.; Pyshnyi, D.; Kharkova, M.; Vlassov, V.; Laktionov, P. Immunochemical assay for deoxyribonuclease activity in body fluids. *J. Immunol. Methods* **2007**, *325*, 96−103.

(29) Bastings, M. M. C.; Anastassacos, F. M.; Ponnuswamy, N.; Leifer, F. G.; Cuneo, G.; Lin, C.; Ingber, D. E.; Ryu, J. H.; Shih, W. M. Modulation of the Cellular Uptake of DNA Origami through Control over Mass and Shape. *Nano Lett.* **2018**, *18* (6), 3557−3564.



https://dx.doi.org/10.1021/jacs.9b11698
J. Am. Chem. Soc. 2020, 142, 3311−3315